STABILITY OF A LIQUID METAL FREE SURFACE IN AN ANNULUS AFFECTED BY AN ALTERNATING MAGNETIC FIELD

J.–U. Mohring, A. Potherat

Department of Electroheat, Technische Universität Ilmenau, P.O.Box 100565, D-98684 Ilmenau, Germany

Introduction. The control of liquid metal free free surfaces by electromagnetic forces is used in many metallurgical processes, including electromagnetic levitation, cold crucible technologies, and electromagnetic slit sealing. The contactless control of free surfaces opens new possibilities in achieving high quality products. The main problem with these technologies is the stability of conducting free surfaces under the influence of electromagnetic fields. In the past many analytical and numerical investigations were performed, e.g., by Belkessam [1], and by Fautrelle and Sneyd [2]. The latter have demonstrated that an instability of a flat conducting free surface sets in when the applied alternating magnetic field exceeds a certain critical value B_c. A special case of this problem which is similar to the process of electromagnetic slit sealing is a free surface in a elongated slit or in an annulus. Experimental and analytical studies were performed by Mohring and Karcher [3, 4]. They characterized several kinds of surface instabilities, and analyzed the dependence of the critical current on relevant parameters. However, the experimental setup only allowed to see a part of free surface, not the full perimeter. The analytical model did not account for the slit thickness. Within this context we present both a new experimental arrangement and a more sophisticated analytical model.

1. Measurements.

1.1. Experimental setup. The apparatus used in the experiment is schematically shown in Fig. 1. It contains an annulus filled with a liquid metal and an inductor which is located at a distance L above the free surface. The annulus walls are made of perspex and can be changed to achieve different gap widths a. The gap between the inner and outer walls is filled with GaInSn (or Galinstan, of melting point –19°C). To prevent the free surface oxidation, the latter is covered

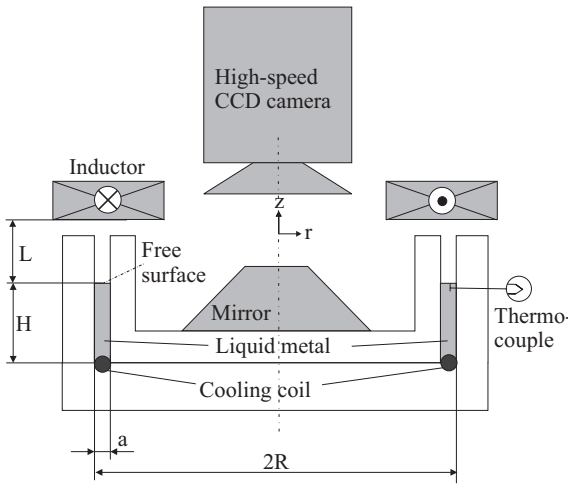

Fig. 1. Experimental setup.

Table 1. Experimental parameters.

Parameter	Dimension	Parameter	Dimension
a	1, 2, 3, 4, 5, 6 mm	H	25 mm
L	16 mm	R	76 mm
f	5 kHz $< f <$ 50 kHz	I	5 kHz $< f <$ 50 kHz

with a thin layer of diluted sodium hydroxide. The electromagnetic field is generated by an inductor made of copper which is fed by an alternating current I of variable frequency f (only in discrete steps).

The alternating magnetic field density B on the free metal surface mainly has a radial component which has two important effects. Due to the limited penetration depth δ_s, the magnetic pressure $p_m = B^2/2\mu$ has a gradient in the axial direction and generates a Lorentz force density in the liquid metal. This force acts in the direction of gravity. The 2^{nd} effect are unwelcome Joule heat losses which lead to a strong temperature increase of the liquid metal, in particular, at the free surface. These losses are only partly removed by the cooling coil located at the bottom of the annulus. Therefore, it is necessary to monitor the temperature of the metal by a thin thermocouple which is located 2 mm under the surface. Inside the annulus a purpose-built mirror is arranged which is made of brass and has a chromium-plated surface layer of a few μm. This device makes it possible to observe the free surface along the whole perimeter at once. A digital high-speed camera (max. resolution 1024^2, used frame rate 77 fps), which is located 25 cm above the mirror, records the movement of the free surface over time. We use the method of digital image processing (DIP) to analyze the surface shape because it is the most accurate method for the applied experimental arrangement. Fig. 2 shows typical pictures recorded by the high-speed camera. A strong light outside the annulus makes a high contrast between the liquid metal and the transparent sodium hydroxide. Using MATLAB the free surface is automatically found and resampled as a periodic function $h(\varphi)$, which is represented by 360 points along the perimeter. The smallest height difference which can be detected with the present method is about 1/6 mm. FFT analysis of $h(\varphi)$ provides the spectrum of existing wave lenghts.

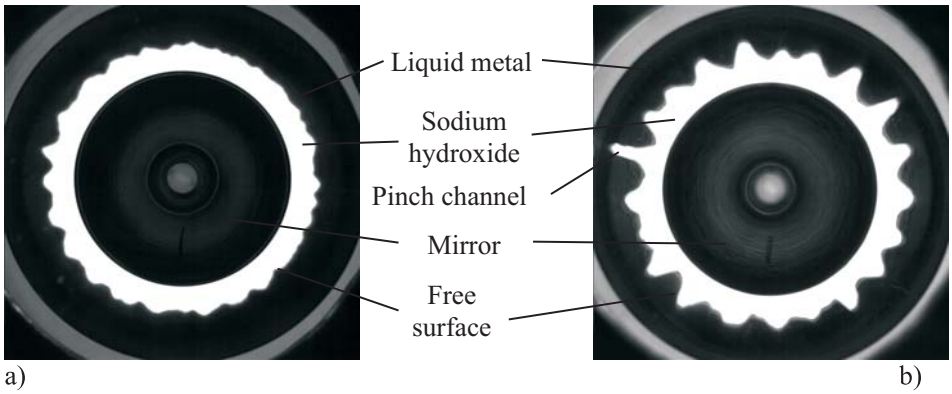

Fig. 2. Surface instabilities: (a) surface waves, (b) pinch effect.

1.2. Experimental results. When increasing the inductor current I from 0, we observe different kinds of surface instabilities in the liquid metal. Up to a certain value of I the free surface does not show any movement. Then small surface waves travelling along perimeter can be seen. When the current reaches a first treshold value, the waves merge into a stable static surface deformation which is characterized by a dominant wave length λ (see Fig. 2*a*). At a slightly higher current an electromagnetic pinch sets in (Fig. 2*b*). In this case the liquid metal height is rapidly decreasing at a certain position of the annulus, and a thin pinch channel is developing. This behavior is well-known from the classic DC pinch effect in a jet [5]. The most important difference between the classic DC pinch and the observed AC pinch is the static surface deformation before the pinch. This is a steady state, and can be hold for a few seconds at a constant current. There are two reasons for this phenomenon. Firstly, the distribution of the current density is increased in the troughs and decreased under the wave maxima. This effect can be observed in numerical simulations. The electromagnetic pressure is, therefore, higher in the throughs, and can compensate both the surface tension and the hydrodynamic pressure. Secondly, the thin layer in which the electric current flows, partly follows the surface displacement instead of being fully compressed by it. This effect prevents the strong increase of the current density like in the jet-case, so the onset of the pinch instability occurs for higher currents.

2. Analytical Model

2.1. Hydrodynamic equations. The hydrodynamic model relies on the incompressible shallow water MHD equations with a moving free surface located at $z = h(\varphi, t)$ at time t. In this framework, the velocity $u\mathbf{e}_\varphi + \mathbf{we_z}$ is assumed to depend on φ and t only, whereas the pressure $p(z, \varphi, t)$ depends also on z. The motion equations are then averaged over the channel height $0 < z < h(\varphi, t)$ using a free surface boundary condition for the velocity:

$$\begin{aligned} \rho\partial_t u = {} & \rho g \frac{1}{R}\partial_\varphi h - \frac{\gamma}{R^3}\partial^3_{\varphi\varphi\varphi} h + \frac{B_s}{\mu}\frac{1}{R}\partial_\varphi B_s \\ & + \frac{1}{2\mu}\frac{1}{h}\frac{1}{R}\partial_\varphi \int_0^h B_r^2 \,\mathrm{d}z - \frac{1}{2\mu}\frac{1}{h}\frac{B_s^2}{R}\partial_\varphi h = 0 \qquad R\partial_t h = -\partial_\varphi(hu) \end{aligned} \tag{1}$$

here the Lorentz force is assumed vertical, and where it is assumed that the pressure at the free surface results from azimuthal surface tension effects for small amplitude surface deformations, i.e., $p\big(h(\varphi), t\big) = -\gamma\partial^2_{\varphi\varphi} h$, where γ is the surface tension between Gallinstan and water.

2.2. Electromagnetic model. Because of the small dimensions and the low velocities involved, the electric current $j\mathbf{e}_\varphi$ and the magnetic field $B\mathbf{e_r}$ are not influenced by the flow directly but depend only on the shape of the free surface (Low magnetic Reynolds number approximation). In this context, the magnetic field at the free surface $B_s = B_r(h)$ is the sum of the magnetic field induced by the inductor B_0 and of that induced by the thin current sheet flowing under the liquid metal surface B_J. The application of Ampère's theorem on a contour around the liquid metal domain in a radial section of the channel yields the relation between the average electric current $\bar{j} = \int_0^h j_\varphi \,\mathrm{d}z$ and B_s. $2(a+\delta)B_J = a\delta\bar{j}$, where a is the radial width of the channel and B_J is assumed constant around the contour and where $\delta(\varphi, t) = 1/B_s \int_0^h B_r \,\mathrm{d}z$ can be seen as a generalized skin depth accounting for the current induced along the vertical walls. Further, assuming that $\bar{j} \approx B_s/\delta$,

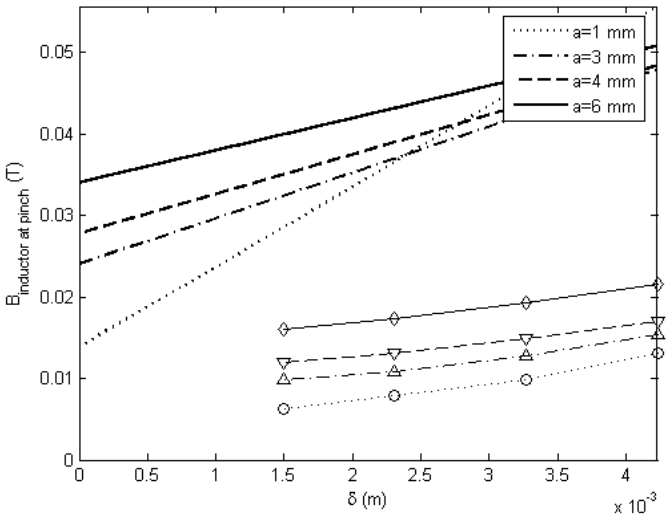

Fig. 3. Magnetic field B_0 at the onset of the pinch instability for several channel widths. The set of curves giving the highest values are obtained from (3).

we get the dependence of the magnetic field on the geometry:

$$\frac{B_s}{B_0} = 2\frac{1+\frac{\delta}{a}}{1+2\frac{\delta}{a}} \tag{2}$$

The final model is obtained by inserting (2) in hydrodynamic equation (1), and approximating $B_r(z)$ by an exponential profile. At equilibrium, $u = 0$, $h = h_0$ and $\delta = \delta_0$.

2.3. Linear stability analysis. We now introduce an infinitesimal perturbation in the obtained model, which can be decomposed in normal modes of the form $[u' = U(t)\exp(k\varphi),\ \delta' = h' = H(t)\exp(k\varphi)]$ due to the symmetries of the problem. The choice of $\delta' = h'$ precludes static waves as observed in the experiment, as those require that $\delta(\varphi)$ and $h(\varphi)$ are different functions. A more precise model could be obtained by introducing independent perturbations in the diffusion equation for the magnetic field. The present simplified model aims only at characterizing the pinch effect. The instability threshold for the magnetic field finally expresses as

$$\frac{B_0^2}{4\mu} > \frac{1}{F(\eta)}\rho g\delta_0 \quad \text{with} \quad F(\eta) = \frac{4\eta(1+\eta)}{(2\eta+1)^2} \quad \text{and} \quad \eta = \frac{\delta}{a}\,. \tag{3}$$

Comparison with the experiment in Fig. 3 reveals the high price we end up paying for the simplified model for the magnetic field (2). The end result (3). however, reproduces well the qualitative dependence on both δ and a of the instability threshold. This suggests to improve the model, for instance, by replacing (2) with a tabulated function obtained from numerical simulations.

REFERENCES

1. O. Belkessam. *Lagestabilisierung von Metallschmelzen mit freier Oberfläche im elektromagnetischen Wechselfeld.* Ph.D. dissertation, Technische Universität Ilmenau, 1998.
2. Y. Fautrelle, A. Sneyd. Instability of a plane conducting free surface submitted to an alternating magnetic field. *J. Fluid Mech.*, vol. 375 (1998), pp. 65–83.
3. Ch. Karcher, J.-U. Mohring. Stability of a liquid metal interface affected by a high-frequency magnetic field. *Magnetohydrodynamics*, vol. 39 (2003), no. 3, pp. 267–276.
4. J.-U. Mohring, Ch. Karcher and D. Schulze. Dynamic behavior of a liquid metal interface under the influence of a high-frequency magnetic field. *Phys. Rev. E*, vol. 71 (2005), no. 1.
5. G. S. Murty. Instability of conducting fluid cylinder due to axial current. *Arkiv för Fysik*, Band 18 (1960), no. 14.